

EFFECTIVE RADIATION AREA OF HUMAN BODY CALCULATED BY A NUMERICAL SIMULATION

**Yoshiichi Ozeki,
Masaaki Konishi**

Asahi Glass Co., Ltd. Research Center,
Kanagawa, Japan

**Chie Narita,
Shin-ichi Tanabe**

Dept. of Human Env. Eng.,
Ochanomizu Univ., Tokyo, Japan

ABSTRACT

A numerical simulation method is developed for predicting the effective radiation area and the projected area of a human body for any postures. This method is based on the solar heat gain simulation for buildings. To confirm the validity of the present method, predicted effective radiation area factors and projected area factors for both standing and seated person are compared with those by the measurements. It was found that predicted values agree quite well with those by the subjective experiments within 10% accuracy. The effective radiation area and the diagrams of the projected area factors for a person sitting on the floor are illustrated.

KEYWORDS

numerical simulation, solar radiation, effective radiation area,
projected area, body posture

1 INTRODUCTION

Non-uniform indoor climate is often observed in a large enclosure such as an atrium and even in a narrow space such as a passenger compartment in a vehicle. In these indoor spaces, conventional thermal indices like SET* and PMV are not considered to be suitable because of non-uniformity. New methods for predicting thermal comfort in non-uniform spaces are highly required. In this paper, a new numerical simulation method is proposed for predicting the effective radiation area and the projected area of a human body for any postures which is based on the solar heat gain simulation proposed by the authors¹⁾. The validity of this method is confirmed by comparison with Fanger's and Underwood's projected area factors obtained by a photographic method for both standing and seated postures. Furthermore, the effective radiation area and the diagrams of the projected area factors for a person sitting on the floor are illustrated. Distribution and intensity of solar radiation to the

human body surface can be predicted with enough accuracy. The present method is proved to be useful tool for predicting them.

2 REVIEW OF PREVIOUS STUDIES

Photographic methods have been applied to calculate the effective radiation area of human body^{2),3),4)}. Underwood et al. measured 19 different types of projected areas for 25 male and female subjects using a photographic method. He proposed an empirical equation for calculating the direct radiation area for a standing posture²⁾. However, there were only for standing and nude subjects. Fanger et al. measured 78 types of the projected area factors (Note 1) for 10 male and female subjects with and without clothing for standing and seated postures using a photographic method. They also calculated the effective radiation area by employing the projected area factors³⁾. Tsuchikawa et al. measured angle factors between standing or sedentary postures and rectangular planes. They also calculated the effective radiation area

by a photographic method⁴). They used orthographic lens for measurements. It must be noted that conventional photographic methods have a limitation in measuring these factors for practical use because of consuming too much time for applying any postures.

Zeng et al. examined the heat transfer characteristics of the human body by a combined numerical simulation of air flow with thermal radiation and moisture transport. Two node model by Gagge is applied to simulate the human body temperature controlling system⁵. Miyazaki et al. verified the angle factors between human body model, which consists of several cylindrical parts, and rectangular planes by Monte Carlo Method⁶. However, their angle factors did not correspond to the Fanger's experimental ones within a sufficient accuracy. There were few studies for calculating the effective radiation area and the projected area for any postures by numerical simulation methods.

3 NUMERICAL SIMULATION METHOD

3.1 Effective radiation area of human body

The effective radiation area of a human body is the surface area of a human body which directly contributes radiation exchange between the body and its surroundings. In case of setting the surroundings as a large sphere with a radius r_m , the effective radiation area of human body A_{eff} is derived in Eq.(1) with the angle factor F_{A2-p} between sphere and human body (Fig.1)³.

$$A_{eff} = 4\pi r_m^2 F_{A2-p} \quad (1)$$

If we calculate the angle factor F_{A2-p} with projected area of human body A_p on a plane perpendicular to the direction of the differential surface element dA_2 on the sphere (Fig.2), the effective radiation area can be derived by surface

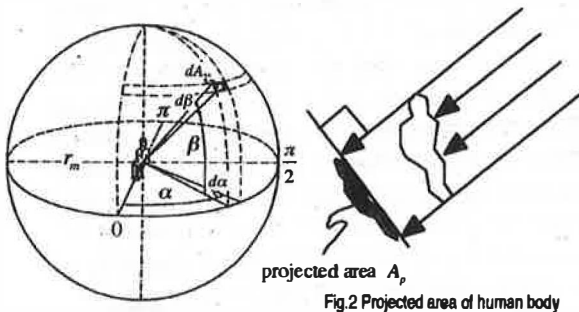


Fig.1 Notation pertinent to calculation of the effective radiation area³⁾

Fig.2 Projected area of human body

integration of projected area with spherical coordinate system³.

$$A_{eff} = \frac{4}{\pi} \int_{\alpha=0}^{\alpha=\pi} \int_{\beta=0}^{\beta=\frac{\pi}{2}} A_p \cos \beta \, d\alpha \, d\beta \quad (2)$$

To derive the projected area factor, Fanger introduced parallel ray method. On the other hand, Tsuchikawa introduced solid angle method. Significant difference in both methods must be appeared in angle factors when surroundings are close to the human body. Solid angle method is more appropriate than parallel ray one under this condition. However, in case of evaluating the solar heat gain, parallel ray method is suitable. Present method can select appropriate one according to the long wave radiation exchange or solar heat gain. However, in this paper, only parallel ray method is introduced because we confirm the validity of a human body model by comparison with measurements by Underwood²) and Fanger³).

3.2 Human body model

The configuration of a human body affects the characteristics of radiation exchange and solar heat gain. Several models are proposed to simulate the heat transfer characteristics around human body^{6),7),8)}. In this paper, a human body model which represents the uneven shape such as ears, nose, mouth, fingers of hands and toes in detail is considered to be suitable to predict heat transfer characteristics as shown in Fig.3 (Note 2). Height of this model and surface areas of each body part are shown in Tables 1 and 2. Height and surface area of the present model are close to the measurements by Fanger. Surface areas of each body part are also close to those proposed by Tanabe, thermal regulation with 16 body parts⁹). Human body surface is divided into 4396 surface elements such as quadrilaterals for both standing and seated postures.

3.3 Projected area of human body

To calculate the effective radiation area of a human body with Eq.(2), the projected area A_p of a human body to the parallel rays must be calculated. This projected area is equal to the surface area of the human body where parallel rays reach directly and which is projected on a

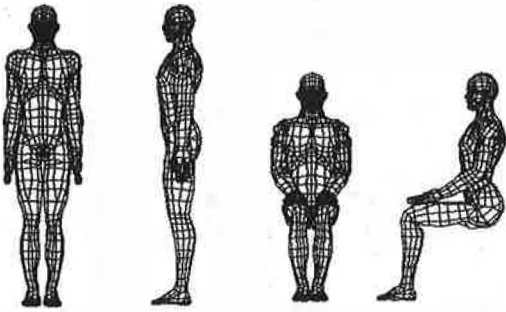


Fig.3. Human body model (standing and seated postures)

Table 1 Height and total surface area of the human body

	Present	Underwood ^{a)}	Fanger ^{b)}	Tsuchikawa ^{c)}	Zeng ^{b)}	Miyazaki ^{b)}
Height (m)	1.75	—	1.72	1.70	1.65	1.71
Total Surface area (m ²)	1.72	1.81	1.74	1.69	1.70	1.58

^{a)}Underwood : mean of 25 male subjects

^{b)}Fanger : mean of 10 male and female subjects

^{c)}Tsuchikawa : mean of 3 male subjects

Table 2 Surface area of each body part

(a) Present model (b) Tanabe's model with 16 body parts (nude)⁹⁾

(a) Present model		(b) Tanabe's model with 16 body parts (nude) ⁹⁾	
head	0.091	head	0.14
neck	0.047	chest	0.16
chest	0.088	back	0.14
left shoulder	0.071	croch	0.21
right shoulder	0.071	left shoulder	0.1
abdomen	0.125	left arm	0.06
croch	0.169	left hand	0.05
left upper arm	0.088	right shoulder	0.1
left forearm	0.059	right arm	0.06
left hand	0.052	right hand	0.05
right upper arm	0.090	left thigh	0.21
right forearm	0.058	left leg	0.11
right hand	0.052	left foot	0.06
left thigh	0.165	right thigh	0.21
left leg	0.112	right leg	0.11
left foot	0.051	right foot	0.06
right thigh	0.165	total	1.83
right leg	0.112		
right foot	0.051		
total	1.715		

unit : m²

plane perpendicular to the parallel rays. This area is calculated by the solar heat gain simulation shown in reference 1.

In the solar heat gain simulation, solar radiation to the walls is calculated in response to the geometry of the room and material property of each wall such as transmissivity and reflectivity. Absorbed solar radiation on each wall is calculated on the basis of incoming solar radiation mentioned above. Solar radiation such as direct, sky-diffused, ground-reflected diffused radiation and multiple reflection of radiation on walls are calculated on the unit of differential surface element by accounting the shade of other walls and outside buildings.

Surface area where parallel rays reach directly is equivalent to the area where solar radiation reaches. These areas are summed as follows. Firstly, body surface is divided into surface elements and these elements are

regarded as non-transmissivity walls. For each surface element, we judged whether there are any other elements which intercepts the sunlight or not. If not, the surface element can receive the sunlight directly. On the other hand, projected area to the projected plane is evaluated by both surface element A_i and incident angle θ_i of the sunlight to the surface element. Thus, the projected area A_p of a human body to the parallel rays is obtained by Eq.(3).

$$A_p = \sum \gamma_i \cos \theta_i A_i \quad (3)$$

γ_i represents whether direct solar radiation reaches the surface element ($\gamma_i = 1$) or not ($\gamma_i = 0$). The algorithm for calculating the projected area of a human body is shown in Fig.4. As the procedure for calculating the solar heat gain can deal with any indoor geometry, this algorithm for calculating the projected area of a human body can also deal with for any postures.

4 VERIFICATION OF EFFECTIVE RADIATION AREA FOR BOTH STANDING AND SEATED POSTURES

To confirm the validity of this method, predicted effective radiation area factors for both standing and seated postures are compared with those by measurements. As for numerical integration of Eq.(2), 91 integration points are set for calculating the effective radiation areas (13 different angles in azimuth α and 7 different angles in altitude β). Calculated effective radiation area and effective radiation area factors are shown in Table 3 (Note 3). Effective radiation area and effective radiation area factor for a standing posture are predicted rather larger

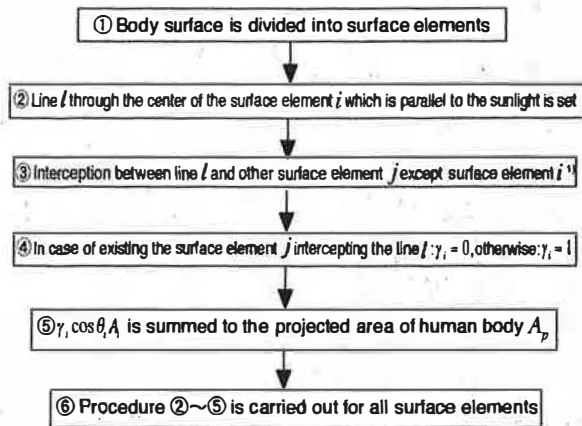


Fig.4. Algorithm for calculating projected area of human body

Table 3 Effective radiation area and effective radiation area factor
(a) standing posture

	Present	Fanger ³⁾	Tsuchikawa ⁴⁾	Miyazaki ⁶⁾
$A_{eff}(m^2)$	1.276	1.262	1.312	1.317
$f_{eff}(-)$	0.744	0.725 ± 0.013	0.803 ± 0.005	0.834

(b) seated posture				
	Present	Fanger ³⁾	Tsuchikawa ⁴⁾	Miyazaki ⁶⁾
$A_{eff}(m^2)$	1.176	1.211	1.214	1.224
$f_{eff}(-)$	0.691	0.696 ± 0.017	0.740 ± 0.012	0.775

*Fanger's results and Tsuchikawa's results : nude

than those for seated. This means a seated posture has about 5% decrease of effective radiation area in radiation exchange between a human body and its surroundings than a standing posture. Predicted results for both standing and seated postures meet quite well with those by the subjective experiments obtained by Fanger.

5 COMPARISON OF PROJECTED AREA FACTORS

5.1 Methods

Firstly, the projected areas for a standing posture in present study were compared with those of experimental results by Underwood²⁾. The dimensionless ratio of the projected area against the total surface area was evaluated for three angles of azimuth α (viz. 0°, 45°, 90°) and various angles of altitude β . Secondly, for a standing posture at an altitude of 0°, the same evaluation was conducted for various angles of azimuth to compare with Fanger's experimental results. Lastly, the effect of a body shape was also evaluated.

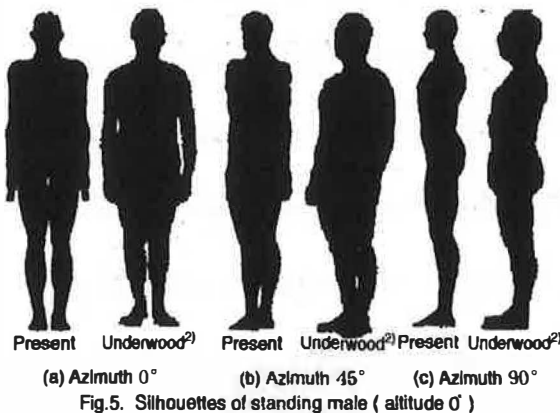


Fig.5. Silhouettes of standing male (altitude 0°)

5.2 Outlines of projected areas

The outlines of projected areas for a standing posture both in present study and in Underwood's one are compared in Fig.5. The difference between two shapes are observed in their shoulders, the size of heads and the location of loins.

5.3 Comparison of projected areas

The dimensionless ratio of the projected area against the total body surface area is shown in Fig.6-(a). At azimuth of 0° and 45°, the projected area gradually decreased according to the rise of altitude. The curve at an azimuth of 90° has its peak around an altitude of 15°, which may be caused by the effect of toes. The maximum value is calculated at an altitude of 0° and an azimuth of 0°.

These results have an almost same tendency as the subjective experimental data by Underwood shown in Fig.6-(b). The biggest difference between two results (5%) is appeared at an altitude of 0° and an azimuth of 0°, which may be caused by the difference of human shapes, especially for shoulders. In the present human model with bigger shoulders than the subjects of Underwood's study, the projected area may be overestimated for azimuth of 0° and 45°. The two results at an azimuth of 90° meet quite well, including the small slope around 80° of altitude.

5.4 Comparison of body shapes

The effect of a human model shape (Note 4) on the projected areas for a standing posture

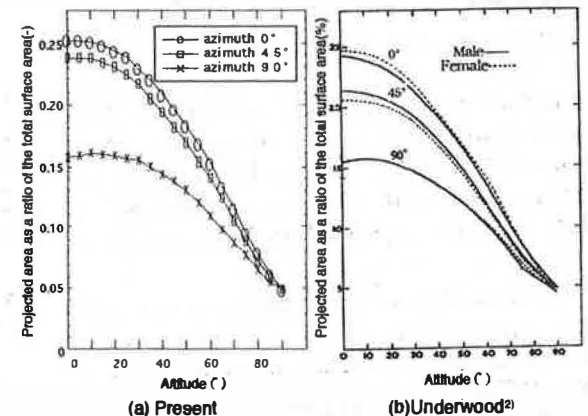


Fig.6. Projected area as a ratio of the total surface area for 3 angles of azimuth

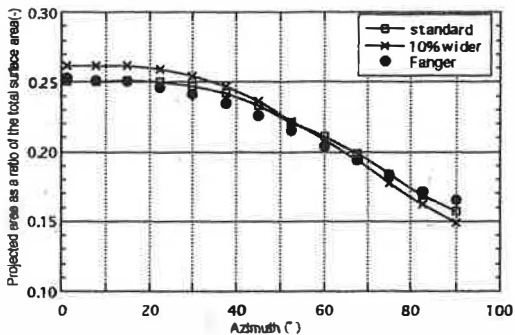


Fig.7. Comparison with projected area at an altitude of 0°

at an altitude of 0° is shown in Fig.7. Comparison is shown for the experimental results by Fanger. Firstly, the present results for a standard body shape have almost constant from 0° to 20° of azimuth, while the experimental results slightly decrease over 30°. It was considered that the outline of present human model from top view is more round than that of Fanger's study. Generally, all results in the present study meet quite well with experimental results.

Secondly, we also compared the difference of body shapes by a new human model wider than a standard model by 10%. The projected area is larger for small angles of azimuth and smaller for large angles of azimuth than a standard model. This tendency can be explained by the change of a body shape.

Furthermore, we tried an another calculation method, using an image processing technique to confirm the accuracy of the present calculation method (Note 5). As shown in Table 4, both results have a good agreement each other.

6 COMPARISON OF PROJECTED AREA FACTORS WITH FANGER'S RESULTS

6.1 Methods

The projected area factors in the present study for both a standing and a sedentary were compared with Fanger's results. Here, the projected area factor is defined as the ratio of the projected area against the effective radiation

Table 4 Comparison of projected area between present method and image processing technique (altitude 0°)

	azimuth 0°	azimuth 45°	azimuth 90°
Present	0.250	0.233	0.157
Image processing technique	0.249	0.234	0.154

(Note) Projected area is normalized by the total surface area

area which is as same as Fanger's study.

6.2 Results

The projected area factors calculated for a standing and a sedentary posture are shown in Fig.8. Comparison is shown for Fanger's experimental results.

For a standing posture, except keeping the constant values at an altitude of 90°, the factors decrease gradually until 90° of azimuth, and then they increase. The curves are almost symmetrical around the azimuth of 90°.

For a sedentary posture, on the other hand, the projected area factors show a wide variation which depends on the altitude. For the angles of 0° and 15° of altitude, there are peaks around 45° and 135° of azimuth, and have a minimum value around 90° of azimuth. These curves are almost symmetrical around 90° of azimuth. For larger altitudes, the symmetrical shape turns gradually to a steady fall, and the value of the projected area factors reduces. The maximum value(0.31) is shown at an azimuth of 30° and at an altitude of 30°, which is more than twice as the minimum one(0.14) at an azimuth of 180° and at an altitude of 60°.

6.3 Comparison of projected area factors

The correlation of the projected area factors between the present results and Fanger's ones is shown in Fig.9. The regressive coefficient and the coefficient of determination in each altitude are shown in Table 5. For a standing posture, the difference of the projected area factors between the altitude of 0° and 15° is very small, as shown in Fig.8-(a). The factors for azimuth ; more than 90° are slightly smaller than those for less than 90° in the range of altitudes over 30°. These tendency correspond to Fanger's experimental results. The present results meet quite well with experimental results for each altitude, which can be proved with total regressive coefficient 1.003 and the coefficient of determination 0.987 in Table 5-(a).

For a sedentary posture, the correlation for the angle of 0° and 15° of altitude is poor, shown in Table 5-(b), which may be caused by the model shape or subjective posture. The total regressive coefficient is 1.002 and the coefficient of determination is 0.891, which show rather

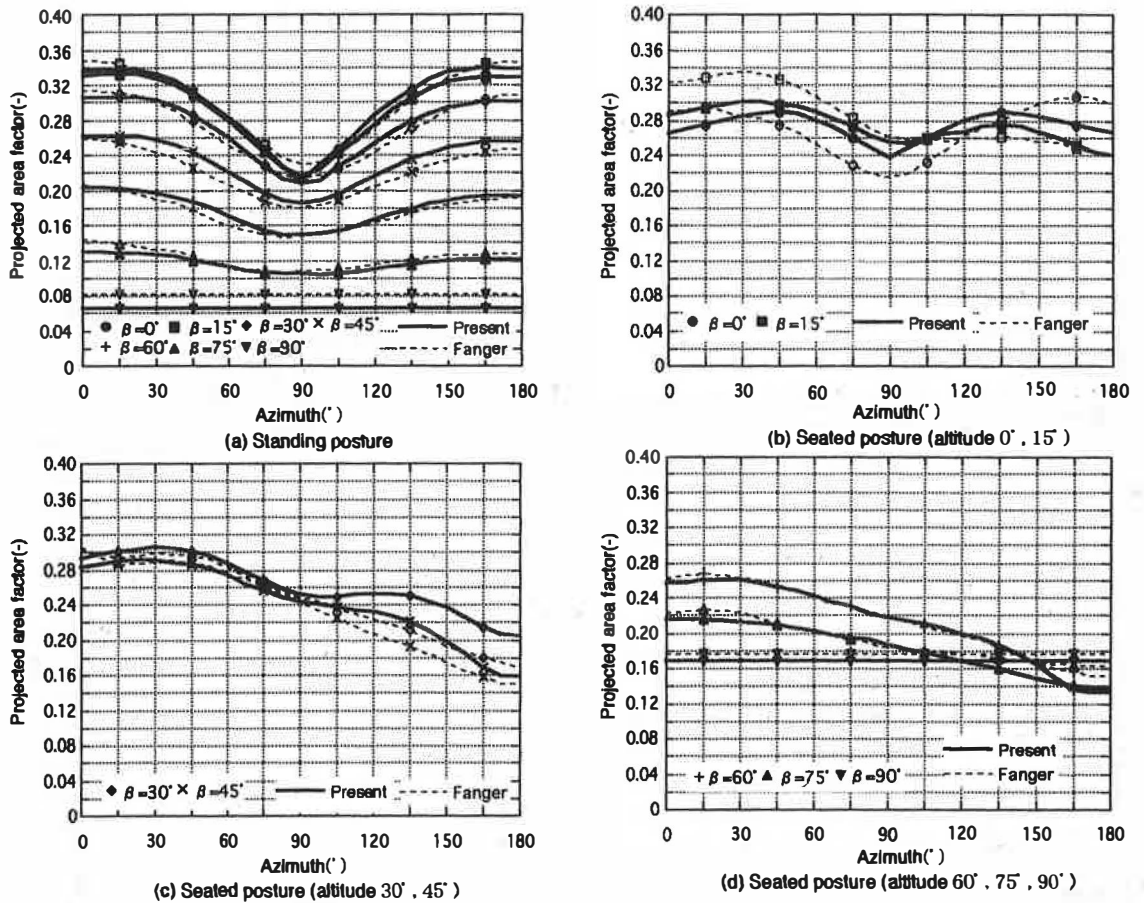


Fig.8. Projected area factor against the effective radiation area (standing and seated postures)

good agreement between two results. Therefore, the present calculated projected area factors meet quite well with those of Fanger's subjective experimental data.

7 EFFECTIVE RADIATION AREA AND PROJECTED AREA FACTORS FOR A PERSON SITTING ON THE FLOOR

7.1 Methods

To show the example of this method, effective radiation area and effective radiation area factors for a person sitting on the floor are calculated. Eq.(2) is predicted by numerical integration as well as section 3. Predicted results are compared with those by the measurements^{10),11)}. Projected area factors are calculated as same method as shown in section 6. The human body model for a person sitting on the floor is shown in Fig.10.

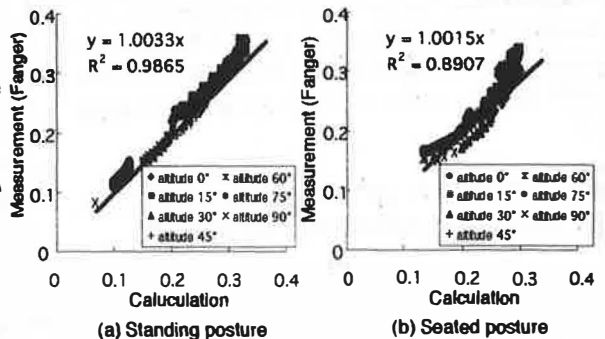


Fig.9. Correlation of the projected area factors between present results and Fanger's

Table 5 Correlation of the projected area factors in each altitude (a) Standing posture

Latitude	0°	15°	30°	45°	60°	75°
Regressive coefficient	1.004	1.025	0.998	0.954	0.982	1.054
Coefficient of determination	0.961	0.974	0.966	0.979	0.961	0.931

(b) Seated posture

Latitude	0°	15°	30°	45°	60°	75°
Regressive coefficient	0.990	1.040	0.944	0.979	1.016	1.042
Coefficient of determination	0.397	0.739	0.846	0.930	0.964	0.796

7.2 Effective radiation area

Predicted effective radiation area and effective radiation area factor are shown in Table 6. Comparison is shown for the measurements. Those factors are smaller than those of both standing and seated postures. This trend corresponds to the previous results by

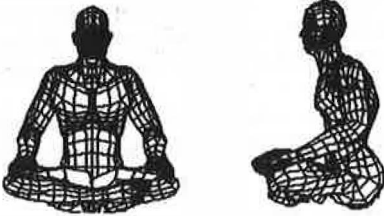


Fig.10. Human body model sitting on the floor

Table 6 Effective radiation area and effective radiation area factor

	Present	Miyamoto ¹⁰⁾	Kakitsuba ¹¹⁾
A_{eff} (m ²)	1.152	1.163	—
f_{eff} (-)	0.662	0.640 ± 0.04	0.675 ± 0.015

*Miyamoto's results : mean of 3 male subjects (nude),
Kakitsuba's results : mean of 2 male subjects (trunks and short-sleeved shirt)

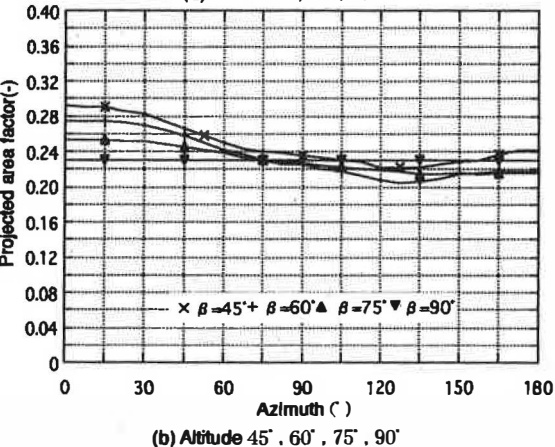
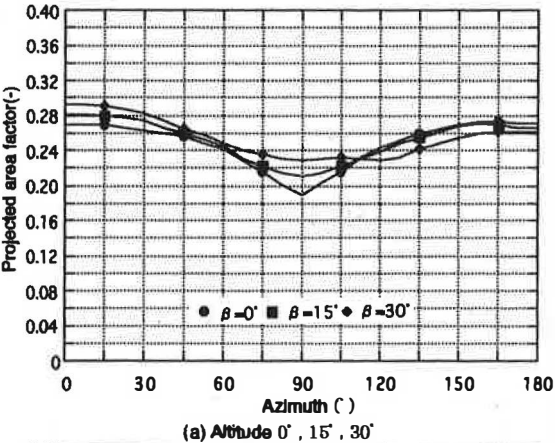


Fig.11. Projected area factor against the effective radiation area (sitting on the floor)

Miyamoto¹⁰⁾. Effective radiation area factor was predicted slightly larger than those of measurement with nude, and smaller than those of the clothed subject with trunks and short-sleeved shirt.

7.3 Projected area factors

The diagram of predicted projected area factors is shown in Fig.11. As well as that of a seated posture, this diagram has a wide variation which depends on the altitude. However, overall trend is similar to that of a seated posture. The difference between minimum and maximum values in projected area factors is smaller than that of a seated posture. One reason is the body shape. A person sitting on the floor is more round than standing and seated ones. Projected area factors around 150° ~ 180° of azimuth is calculated larger than those of seated posture, which is caused by the spreading legs for a sitting person on the floor.

8 CONCLUSIONS

1) A numerical simulation method is proposed for predicting the effective radiation area and the projected area of a human body for any postures on the basis of the solar heat gain simulation.

2) Effective radiation area and effective radiation area factors for both standing and seated persons meet quite well with those by the subjective experiments by Fanger.

3) Predicted projected area factors for a standing person in each angle are compared with those of Underwood. Maximum 5% difference of projected area factors at an altitude of 0° and an azimuth of 0° is observed. However, present model gives a satisfactory accuracy of projected area factors.

4) Comparing the shapes of a standard and 10% wider human body model, maximum 7% difference is observed in the projected area factors. As well as Fanger's results, no significant difference is found between two shapes.

5) Appropriate results for both standing and seated postures can be obtained in projected area factors by comparing with measurements obtained by Fanger.

6) Effective radiation area and effective radiation area factors are predicted for a person

sitting on the floor. Effective radiation area is predicted smaller than those of standing and seated postures as well as the subjective experiments.

7) This model can deal with projected area and effective radiation area for any postures including the evaluation of each body part. Distribution and intensity of solar radiation to the human body surface can be predicted with enough accuracy. The present method is proved to be useful tool for predicting them.

ACKNOWLEDGMENTS

This study has been supported by Mr. M. Ono and Mr. K. Sato of Asahi Glass Co. Ltd.. We would like to express our great gratitude for their cooperation to conduct this study.

NOTES

- 1) The dimensionless ratio of the projected area A_p against the effective radiation A_{eff} ($f_p = A_p / A_{eff}$).
- 2) Present human body model can deal with any postures, a sex difference and body shapes.
- 3) The dimensionless ratio of the effective radiation area A_{eff} against the total surface area A_{tot} ($f_{eff} = A_{eff} / A_{tot}$).
- 4) The human shape is only 10% wider to the width direction of human body than standard one. The total surface area is 1.83 m², and the effective radiation area is 1.38 m².
- 5) Projected area factor is calculated by the pixel of human body projected on the CRT screen and total pixels of CRT screen.

REFERENCES

- 1) Ozeki Y., Sonda Y., Hiramatsu T., Saito T. and Ohgaki S., "Study on Solar Heat Gain Simulation for Coupled Analysis of Radiative and Convective Heat Transfer under Complicated Geometry with Fine Mesh", Transactions of SHASE (The Society of Heating Air-Conditioning and Sanitary Engineers of Japan), No.68, pp.1-11, 1997.
- 2) Underwood C.R. and Ward E.J., "The Solar Radiation Area of Man", ERGONOMICS, Vol.9, No.2, pp.155-168, 1966.
- 3) Fanger P.O., Angelius O., Kjerul P. and Jensen F., "Radiation Data for the Human Body", ASHRAE Transactions, Vol.76- II, pp.338-373, 1970.
- 4) Tsuchikawa T., Kobayashi Y., Horikoshi T., Miwa E., Kurazumi Y. and Hirayama K., "The Effective Radiation Area of the Human Body and Configuration Factors between Human Body and Rectangular Planes and Measured by the Photographic Method", Journal of Archit. Plann. Environ. Engng. AIJ., No.388, pp.48-59, 1988.
- 5) Zeng J., Murakami S. and Kato S., "Coupled simulation of CFD, Radiation and Moisture Transport for Sensible and Latent Heat Loss from Human Body", SEISAN-KENKYU, Monthly Journal of IIS, University of Tokyo, Vol.50, No.1, pp.78-85, 1998.
- 6) Miyazaki Y., Saito M. and Seshimo Y., "A Study of Evaluation of non-uniform Environments by Human Body Model", J. Human and Living Environment, Vol.2, No.1, pp.92-100, 1995.

- 7) Iwamoto S., "Numerical Prediction of Indoor Thermal Environments with Floor Panels based on Radiating Model of Human Body", The 19th Symposium on Human-Environment System, pp.94-97, 1995.
- 8) Yokoyama S., Kakuta N., Tomigashi T., Hamada Y., Nakamura M. and Ochitaji K., "Development of Human Thermal Model in Steady State Expressing Local Characteristic of Each Segment and its Applications", Annual Meeting of SHASE, pp.513-516, 1997.
- 9) Tanabe S., "Numerical model with 16 parts for evaluating non-uniform thermal environment", Annual Meeting of SHASE, pp.457-460, 1994.
- 10) Miyamoto S., Taniguchi Y., Sik C.Y., Tsuchikawa T. and Horikoshi T., "Configuration Factor in case of Radiant Transfer is Blocked by the Human Body Sitting on the Floor", Journal of Archit. Plann. Environ. Engng. AIJ., No.497, pp.33-38, 1997.
- 11) Kakitsuba N. and Suzuki K., "Estimation on Clothing Area Factor as Related to Clothing Microenvironment Volume", Annual Meeting of AIJ, pp.407-408, 1997.

Nomenclature

- A_{eff} : effective radiation area of a human body [m²]
 A_i : area of differential surface element i [m²]
 A_p : projected area of a human body [m²]
 $F_{\Omega-s-p}$: angle factor between sphere and human body [-]
 dA_2 : differential surface element on the sphere [m²]
 i, j : element number [-]
 r_m : a radius of a large sphere [m]
 α : azimuth angle [°]
 β : altitude angle [°]
 γ_i : flag indicating whether the rays reach the surface element i or not [-]
 θ_i : incident angle of the rays to the surface element i [°]